Offshore Container Crane Systems with Robust Optimal Sliding Mode Control

R. M. T. Raja Ismail [a], Nguyen D. That[a,b] and Q. P. Ha [a]

[a]Faculty of Engineering and Information Technology, University of Technology, Sydney, NSW 2007, Australia
[b]Faculty of Marine Electrical and Electronics Engineering, Vietnam Maritime University,Vietnam
E-mail: Raja.RajaIsmail@uts.edu.au; thatkd@vimaru.vn; Quang.Ha@uts.edu.au

Abstract -

Open-sea ship-to-ship transfer operation is an alternative way to avoid port congestion. This process involves a relatively small vessel which transports containers between the harbour and a large cargo ship equipped with a container crane. However, the presence of disturbances and uncertainties caused by harsh open-sea conditions can produce an excessive sway to the hoisting ropes of the crane system. This paper addresses the problem of robust sliding mode control for offshore container crane systems subject to bounded disturbances and uncertain parameters. The mathematical model of an offshore container crane is first derived whereas the effects of ocean waves and gusty winds are taken into account. Then, based on the linear quadratic regulator (LQR) design, a sliding surface is obtained to meet the required performance and stable dynamics for the closed-loop system. Finally, a robust sliding mode controller is proposed to drive the state trajectories of the offshore container crane system towards the sliding surface in finite time and maintain them subsequently on that surface. Simulation results are given to show that the proposed controller can significantly suppress the effects of uncertainties and disturbances from the vessel's wave- and wind-induced motion and wind drag force on the payload.

Keywords -

Sliding mode control, Offshore crane, Ocean wave, Gusty wind, Lyapunov, Linear Quadratic Regulator (LQR).

1 Introduction

Recently, along with rapid developments of the logistics industry, port congestion becomes a major issue all around the world due to the explosive increase in the trading volume [1, 2]. To solve this problem, some ambitious plans of port expansion have been proposed. However, it can be seen that expanding outwards is not a feasible option due to land constraints [3]. Consequently, a new method of transportation, the so-called ship-to-ship cargo transfer operation, is introduced [4]. This operation involves the transfer of containers between a huge container ship and a relatively smaller ship, known as a mobile harbour by using an offshore crane mounted on the container ship [5]. This method, emerging to become a promising solution to improve the port's efficiency and productivity and reduce the operational cost, could enable the ports to stay competitive [6]. For this, the offshore container crane system has to meet stringent safety and efficiency requirements since open-sea waves, winds, and ocean currents easily cause the vessel to move away from a desired position both horizontally and vertically. Therefore, the design of the crane controller is a challenging problem due to the presence of parameter variations and disturbances, e.g. changes of load during the stevedoring operation, from wave- and wind-induced vibrations. These seriously affect the control system performance.

During the past decade, several control schemes have been developed to improve the crane operation performance such as input shaping control [7, 8], optimal control [9, 10] and fuzzy control [11]. However, conventional control methods, applied for crane systems in general, are inapplicable to offshore cranes which are subject to variations in the system matrices due to the changes of the payload mass and rope length and wave- and wind-induced disturbances of a large amplitude. To ensure the safety and reliability of offshore container crane operation, it is necessary to mitigate the effects of these uncertainties and disturbances.

Sliding mode control (SMC) has been recognised as a strong control methodology for the Lagrangian systems, for example the robotic excavator [12], construction robot [13], and tunneling shield machine [14]. The SMC design begins with the selection of a stable sliding surface with desired performance characteristics. Then, the discontinuous control is designed to drive the state trajectory towards the sliding surface and maintain it on this surface over time. The dynamic characteristics of the resulting closed-loop control system will be equivalently determined by the sliding surface design. In [5], the model of an offshore container crane was first introduced where the length of the hoisting rope was considered as a constant. Then, an extended mathematical model was developed in [15] by taking into account the variation of the rope length. For this, a second-order sliding mode controller was also proposed to deal with the problem of trajectory tracking of the crane trolley position and its hoisting rope length. Recently, a further improved result was reported in [16] by considering the offshore crane control problem in three dimensions. However, there remain interesting questions as to how to deal with the payload mass, rope length variation and input disturbances due to nonlinear frictions, strong waves and gusty winds which can significantly affect the payload sway angle of offshore cranes and their safe operations.

In this paper, the problem of robust sliding mode control is investigated for offshore container crane systems with bounded disturbances and uncertainties. Here, based on the dynamics analysis, the mathematical model of the ship-mounted container crane subject to parameter variations and disturbances, is derived for the first time. By utilizing the LQR design approach, a desired sliding surface is obtained. A robust sliding mode controller is then synthesized to drive the state trajectories of the closed-loop system towards the sliding surface in finite time and maintain it there after subsequent time. Simulation results are given to illustrate the feasibility of the proposed approach in terms of reducing the effects of uncertainties and disturbances caused by the changes in payload mass, length of rope and also the vibration effects of ocean waves and gusty winds.

2 Modelling and Problem Statement

The offshore container crane system considered in this study consists of a gantry crane mounted on a ship vessel as visualize in Figure 1, where $\{O_0x_0y_0z_0\}$ and $\{O_Bx_By_Bz_B\}$ are the coordinate frames respectively of the ground and the vessel. The offshore crane system motion is represented by three generalized coordinates; in which, y is the position of the cart, l is the length of the rope, θ is the sway angle induced by the motion of the cart, h is the vertical position of the cart, and m_c and m_p are respectively the masses of the cart and the payload. Let $\zeta(t)$ be the heaving and $\alpha(t)$ be the rolling angular displacement of the vessel. Thus, the position vectors of the cart and the payload with respect to the vessel coordinate frame $\{O_Bx_By_Bz_B\}$ are

$$p_B^c = [y, h]^T, \quad p_B^m = [y + l\sin\theta, h - l\cos\theta]^T.$$

The position vectors of the cart and the payload with respect to the ground coordinate frame $\{O_0x_0y_0z_0\}$ can be obtained by multiplying the augmented position vectors with a homogeneous transformation matrix. Let $\hat{p}_B^c$ and $\hat{p}_B^m$ are respectively the augmented position vectors of p_B^c and p_B^m such that

$$\hat{p}_B^c = [(p_B^c)^T, 1]^T, \quad \hat{p}_B^m = [(p_B^m)^T, 1]^T.$$

Hence, the augmented position vectors of the cart and the payload with respect to $\{O_0x_0y_0z_0\}$ are given by

$$\hat{p}_0^c = T_0^B\hat{p}_B^c, \quad \hat{p}_0^m = T_0^B\hat{p}_B^m,$$

where $\hat{p}_0^c = [(p_0^c)^T, 1]^T$, $\hat{p}_0^m = [(p_0^m)^T, 1]^T$ and

$$T_0^B = \begin{bmatrix} \cos\alpha & \sin\alpha & 0 \\ -\sin\alpha & \cos\alpha & \zeta \\ 0 & 0 & 1 \end{bmatrix}.$$

Thus, the kinetic energy, potential energy and Lagrangian of the crane system are obtained respectively as

$$\begin{aligned} \mathcal{K} =& \frac{1}{2}m_c\|\dot{p}_0^c\|^2 + \frac{1}{2}m_p\|\dot{p}_0^m\|^2, \\ \mathcal{P} =& m_cg(p_0^c)_z + m_pg(p_0^m)_z, \\ \mathcal{L} =& \mathcal{K} - \mathcal{P}, \end{aligned}$$

where $(\cdot)_z$ denotes the z-component of the vector. By applying the Euler-Lagrange formulation

$$\frac{d}{dt}\left(\frac{\partial\mathcal{L}}{\partial\dot{q}_i}\right) - \frac{\partial\mathcal{L}}{\partial q_i} = \tau_i, \quad i = 1, 2, 3$$

the dynamic model of the offshore crane system can be obtained in the following form:

$$M(q)\ddot{q} + f(q, \dot{q}) + \Delta f(t, q, \dot{q}) = \tau(t) - \tau_c(t), \tag{1}$$

where $q = [y, l, \theta]^T \in \mathbb{R}^3$ is the vector of generalized coordinates and $\tau(t) = [F_y(t), F_l(t), 0]^T \in \mathbb{R}^3$ is the vector of input forces. In (1), $M(q) \in \mathbb{R}^{3\times3}$ is the inertia matrix, $f(q, \dot{q}) \in \mathbb{R}^3$ is the vector of centrifugal-Coriolis and gravity forces, $\Delta f(t, q, \dot{q}) \in \mathbb{R}^3$ is the vector of disturbances in the system due to open-sea wave-induced vibrations, and $\tau_c(t) \in \mathbb{R}^3$ is the vector of disturbances due to Coulomb friction and wind drag force on the payload.

The system matrices are derived as follows:

$$\begin{aligned} M(q) &= \begin{bmatrix} m_c + m_p & m_p\sin\theta & m_pl\cos\theta \\ m_p\sin\theta & m_p & 0 \\ m_pl\cos\theta & 0 & m_pl^2 \end{bmatrix}, \\ f(q, \dot{q}) &= \begin{bmatrix} 2m_p\dot{l}\dot{\theta}\cos\theta - m_pl\dot{\theta}^2\sin\theta + K_{cy}\dot{y} \\ -m_pl\dot{\theta}^2 - m_pg\cos\theta + K_{cl}\dot{l} \\ 2m_pl\dot{l}\dot{\theta} + m_pgl\sin\theta + K_{c\theta}\dot{\theta} \end{bmatrix}, \\ \Delta f(t, q, \dot{q}) &= \left[\Delta f_1, \Delta f_2, \Delta f_3\right]^T, \\ \tau_c(t) &= \begin{bmatrix} F_{cy}\,\mathrm{sign}\,\dot{y} \\ F_{cl}\,\mathrm{sign}\,\dot{l} \\ \tau_{c\theta}\,\mathrm{sign}\,\dot{\theta} + \tau_{wd}(t)\sin 2\pi f_wt \end{bmatrix}, \end{aligned}$$

where

$$\begin{aligned} \Delta f_1 =& (m_c + m_p)\left(-y\dot{\alpha}^2 + h\ddot{\alpha} - (g + \ddot{\zeta})\sin\alpha\right) \\ &+ 2m_p(l\dot{\theta}\dot{\alpha}\sin\theta - \dot{l}\dot{\alpha}\cos\theta) \\ &- m_pl\left(\sin\theta\dot{\alpha}^2 + \cos\theta\ddot{\alpha}\right), \\ \Delta f_2 =& m_p\Big[(y\cos\theta + h\sin\theta)\ddot{\alpha} + 2\dot{y}\dot{\alpha}\cos\theta + 2l\dot{\theta}\dot{\alpha} \\ &- (y\sin\theta - h\cos\theta + l)\dot{\alpha}^2 + g\cos\theta \\ &- (g + \ddot{\zeta})\cos(\theta - \alpha)\Big], \\ \Delta f_3 =& m_p\Big[-2l\dot{l}\dot{\alpha} - 2\dot{y}\dot{\alpha}l\sin\theta - (yl\sin\theta - hl\cos\theta \\ &- l^2)\ddot{\alpha} - gl\sin\theta + l(y\cos\theta + h\sin\theta)\dot{\alpha}^2 \\ &+ (g + \ddot{\zeta})l\sin(\theta - \alpha)\Big], \end{aligned}$$

in which K_{cy}, K_{cl} and $K_{c\theta}$ are the viscous friction coefficients, and F_{cy}, F_{cl} and $\tau_{c\theta}$ are the Coulomb friction coefficients. The term $\tau_{wd}(t)$ represents the magnitude of the torque produced by the wind drag force on the payload and it can be calculated by using the following formula [17]:

$$\tau_{wd}(t) = \frac{1}{2}\rho_wv_w^2c_dA_p[l(t) + L_c],$$

where ρ_w is the density of air, v_w is the velocity of the wind, c_d is the drag coefficient, A_p is the effective surface area of the payload, and L_c is the average distance from the hook to the payload center of gravity.

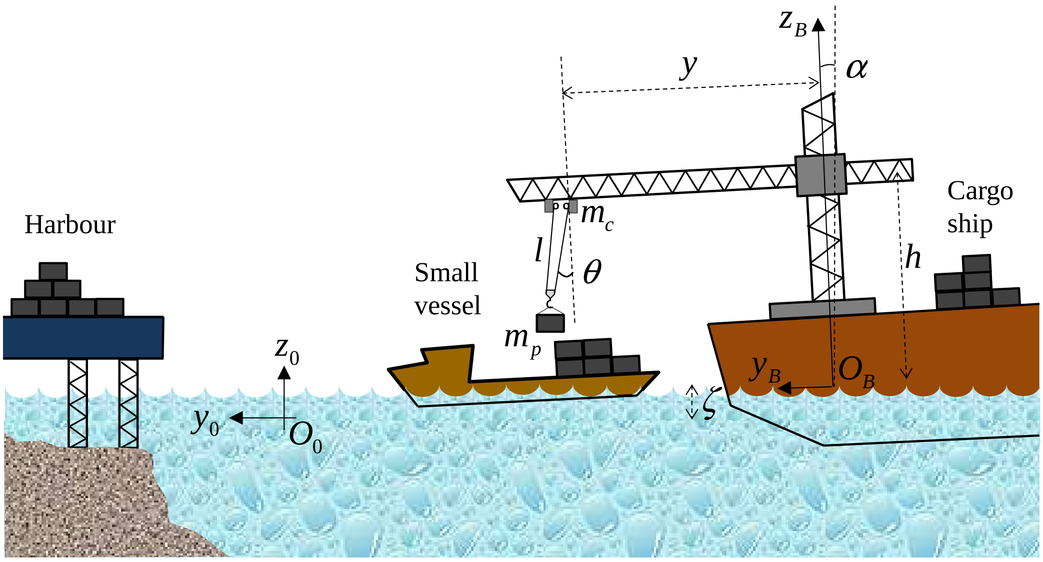

Figure 1: Motion of the offshore crane during containers transfer operation.

System (1) is a typical underactuated system since the number of control inputs is less than the number of generalized coordinates. Thus, we can partition the vector of generalized coordinates into actuated and unactuated parts, such that $q = [q_a^T, q_u^T]^T$, where $q_a = [y, l]^T$ and $q_u = \theta$. It follows that, the matrices and vectors in (1) can be partitioned as

$$M(q) = \begin{bmatrix} M_{aa} & M_{au} \\ M_{au}^T & M_{uu} \end{bmatrix}, f(q, \dot{q}) = \begin{bmatrix} f_a \\ f_u \end{bmatrix},$$
$$\Delta f(t, q, \dot{q}) = \begin{bmatrix} \Delta f_a \\ \Delta f_u \end{bmatrix}, \tau(t) = \begin{bmatrix} u_a(t) \\ 0 \end{bmatrix}, \tau_c(t) = \begin{bmatrix} \tau_{ca}(t) \\ \tau_{cu}(t) \end{bmatrix}.$$

The sub-blocks of the above matrices and vectors are obtained based on the dimensions of vectors q_a and q_u.

For the purpose of control design, we introduce a state variable vector $x \in \mathbb{R}^6$ as

$$x = [x_1, x_2, x_3, x_4, x_5, x_6]^T = [y, l, \theta, \dot{y}, \dot{l}, \dot{\theta}]^T.$$

Hence, by substituting $[q^T, \dot{q}^T]$ in system (1) with the state vector x, the offshore container crane dynamics can be expressed in the state-space as follows:

$$\dot{x} = F(x) + \Delta F(t, x) + G(x)u_a(t) + H(x)\omega(t), \quad (2)$$

where

$$F(x) = \begin{bmatrix} x_4 \\ x_5 \\ x_6 \\ \overline{f}_a \\ -M_{uu}^{-1}(M_{au}^T \overline{f}_a + f_u) \end{bmatrix},$$

$$\Delta F(x) = \begin{bmatrix} 0_{3\times1} \\ \Delta\overline{f}_a \\ -M_{uu}^{-1}(M_{au}^T \Delta\overline{f}_a + \Delta f_u) \end{bmatrix},$$
$$G(x) = \begin{bmatrix} 0_{3\times2} \\ \overline{M}^{-1} \\ -M_{uu}^{-1} M_{au}^T \overline{M}^{-1} \end{bmatrix},$$
$$H(x) = \begin{bmatrix} 0_{3\times2} & 0_{3\times1} \\ H_{21} & H_{22} \\ H_{31} & H_{32} \end{bmatrix},$$
$$u_a(t) = \begin{bmatrix} u_1(t) \\ u_2(t) \end{bmatrix} = \begin{bmatrix} F_y(t) \\ F_l(t) \end{bmatrix},$$
$$\omega(t) = \tau_c(t),$$
$$\overline{M} = M_{aa} - M_{au} M_{uu}^{-1} M_{au}^T,$$
$$\overline{f}_a = -\overline{M}^{-1} \left(f_a - M_{au} M_{uu}^{-1} f_u \right),$$
$$\Delta\overline{f}_a = -\overline{M}^{-1} \left(\Delta f_a - M_{au} M_{uu}^{-1} \Delta f_u \right),$$
$$H_{21} = -\overline{M}^{-1},$$
$$H_{22} = \overline{M}^{-1} M_{au} M_{uu}^{-1},$$
$$H_{31} = M_{uu}^{-1} M_{au}^T \overline{M}^{-1},$$
$$H_{32} = -M_{uu}^{-1} \left(M_{au}^T \overline{M}^{-1} + 1 \right).$$

The linearised dynamic model of the offshore crane system (2) about an operating point (x_0, u_0) can be obtained in the form of

$$\dot{\overline{x}}(t) = (A + \Delta A(t))\overline{x}(t) + Bu(t) + D\omega(t), \quad (3)$$

where $\overline{x}(t) = x(t) - x_0$ and $u(t) = u_a(t) - u_0$. By choosing $x_0 = [y_0, l_0, 0, 0, 0, 0]^T$, the state vector of the local model can be represented as $\overline{x}(t) = [\Delta y, \Delta l, \theta, \dot{y}, \dot{l}, \dot{\theta}]^T$, and u_0 can be found as

$$u_0 = -G^\dagger(x_0)F(x_0),$$

in which $G^\dagger$ denotes the Moore-Penrose pseudo-inverse of matrix G. Thus, the system matrix, the input matrix, and the unmatched disturbance matrices are obtained as follows:

$$\begin{aligned} A &= \frac{\partial F(x)}{\partial x} + \sum_{j=1}^{2} \frac{\partial G_j(x)}{\partial x} u_j \bigg|_{\substack{x=x_0 \\ u=u_0}}, \\ B &= G(x_0), \\ \Delta A(t) &= \frac{\partial \Delta F(t,x)}{\partial x} \bigg|_{x=x_0}, \\ D &= H(x_0), \end{aligned}$$

where G_j $(j = 1, 2)$ denotes the jth column of matrix G.

3 Control Design

In this section, a robust sliding mode control scheme is proposed to deal with the problem of trajectory tracking of the crane system whereas the the effects of the ocean waves and gusty winds is mitigated.

3.1 Crane trajectory

For the desired trajectory of the offshore container crane, we assume that there are three stages:

Stage 1 (*Picking up the container with time* t_1): The hoisting rope length decreases from l_D, where the container is on the deck of the large ship to l_U where the container is in the upper position with a maximum lateral velocity v_R. Thus, we have

$$t_1 = \frac{l_D - l_U}{v_R}.$$

It should be noted that the rope length l_D and l_U are assumed to be constant between the different containers.

Stage 2 (*Placing the container on the smaller ship with time* t_1): The rope length increases from l_U to l_D. This is the reverse process for lifting the container.

Stage 3 (*Moving the container with a maximum longitudinal velocity* v_y): Assuming the whole distance of travel of lifting, moving and placing the container is y_F with the corresponding time t_F, the placing phase then will take a time of $t_F - 2t_1$. Denote $y, \dot{y}, l, \dot{l}$ are longitudinal position, velocity of the container and the rope length, its rate of change respectively. We have the following diagrams, from which desired trajectories y_d and l_d can be derived from given parameters l_D, l_U, v_r, v_y, y_F. Desired trajectories of position and velocity of the container are obtained respectively as

$$y_d(t) = \begin{cases} \frac{1}{2}at^2, \;\; 0 \le t \le t_1, \\ v_y t - v_y \frac{t_1}{2}, \;\; t_1 \le t \le t_2, \\ -\frac{1}{2}at^2 + v_y \frac{t_F}{t_1} t + y_F - \frac{1}{2}at_F^2, t_2 \le t \le t_F, \end{cases}$$

$$\dot{y}_d(t) = \begin{cases} at, \;\; 0 \le t \le t_1, \\ v_y, \qquad t_1 \le t \le t_2, \\ -at + v_y \frac{t_F}{t_1}, \;\; t_2 \le t \le t_F, \end{cases}$$

where $a = \frac{v_y}{t_1}, t_2 = t_F - t_1$.

Similarly, desired trajectories of the hoisting rope length and its rate of change are

$$l_d(t) = \begin{cases} -\frac{1}{2}bt^2 + l_D, \;\; 0 \le t \le \frac{t_1}{2}, \\ \frac{1}{2}bt^2 - 2v_R t + v_R t_1 + l_U, \;\; \frac{t_1}{2} \le t \le t_1, \\ l_U, t_1 \le t \le t_2, \\ \frac{1}{2}bt^2 - bt_2 t + \frac{v_R}{t_1} t_2^2 + l_U, \;\; t_2 \le t \le t_F - \frac{t_1}{2}, \\ -\frac{1}{2}bt^2 + bt_F t - \frac{1}{2}bt_F^2 + l_D, \; t_F - \frac{t_1}{2} \le t \le t_F, \end{cases}$$

$$\dot{l}_d(t) = \begin{cases} -bt, \;\; 0 \le t \le \frac{t_1}{2}, \\ bt - bt_1, \;\; \frac{t_1}{2} \le t \le t_1, \\ 0, \;\; t_1 \le t \le t_2, \\ bt - bt_2, \;\; t_2 \le t \le t_F - \frac{t_1}{2}, \\ -bt + bt_F, \;\; t_F - \frac{t_1}{2} \le t \le t_F, \end{cases}$$

where $b = \frac{2v_R}{t_1}$.

3.2 Problem statement

Let us consider a reference model as follows:

$$\dot{x}_d(t) = A_d x_d(t) + B_d r_d(t),$$

where $x_d(t) = [y_d, l_d, \theta_d, \dot{y}_d, \dot{l}_d, \dot{\theta}_d]^T$ and $r_d(t) \in \mathbb{R}^2$ is the bounded reference input. The matrices A_d and B_d are designed in a way that there exist compatibly dimensioned matrices K and L to satisfy the matching condition:

$$\begin{aligned} BK &= A_d - A, \\ BL &= B_d. \end{aligned}$$

Define a tracking error state x_e as the difference between the plant and the reference model state responses:

$$x_e = \overline{x}(t) - x_d(t).$$

Consequently, the following state-space equation with the state vector error is obtained as

$$\begin{aligned} \dot{x}_e(t) =& A_d x_e(t) + (A - A_d)\overline{x}(t) + \Delta A \overline{x}(t) + Bu(t) \\ &- B_d r_d(t) + D\omega(t). \end{aligned} \tag{4}$$

For the purpose of sliding surface design, a transformation matrix $T \in \mathbb{R}^{6\times6}$ is introduced such that

$$TB = \begin{bmatrix} 0 \\ B_2 \end{bmatrix}$$

where $B_2 \in \mathbb{R}^{2\times2}$ is nonsingular. By using the coordinate transformation $z = T\overline{x}$, (4) can be rewritten in the form of the new coordinate:

$$\begin{aligned} \dot{e}(t) =& \overline{A}_d e(t) + (\overline{A} - \overline{A}_d)z(t) + \Delta\overline{A}z(t) + \overline{B}u(t) \\ &- \overline{B}_d r_d(t) + \overline{D}\omega(t), \end{aligned} \tag{5}$$

where $e = Tx_e$, $\overline{A} = TAT^{-1}$, $\Delta\overline{A} = T\Delta AT^{-1}$, $\overline{A}_d = TA_dT^{-1}$, $\overline{B} = TB$, $\overline{B}_d = TB_d$ and $\overline{D} = TD$.

Without loss of generality, we assume that the disturbance $\omega(t)$ and the system uncertainty $\Delta\overline{A}(t)$ are norm-bounded as

$$\|\omega(t)\| \le \overline{\omega}_p, \quad \|\Delta\overline{A}(t)\| \le \beta,$$

where $\overline{\omega}_p, \beta$ are known positive scalars.

Our purpose is first to design a stable sliding surface using the linear quadratic regulator design approach to mitigate the effects of the ocean waves and gusty winds on the system state. Then, a robust sliding mode controller is synthesized to guarantee that the system sliding motion converges exponentially to a ball whose radius and the rate of exponential convergence can be chosen arbitrarily.

3.3 Sliding surface

The sliding function is defined in terms of trajectory tracking errors as follows

$$s(t) = [s_1(t), s_2(t)]^T = \overline{C}e(t) = -Ce_1(t) + e_2(t), \quad (6)$$

where C is a constant matrix to be designed. Consider the following quadratic performance index

$$J = \tfrac{1}{2}\int_{t_s}^{\infty} e^T(t)Qe(t)dt, \quad (7)$$

where $Q = \begin{bmatrix} Q_{11} & Q_{12} \\ Q_{21} & Q_{22} \end{bmatrix}$ is a given symmetric positive definite matrix and t_s is the starting time which indicates the induction of the sliding motion. By noting that

$$\begin{aligned} &2e_1^T(t)Q_{12}e_2(t) + e_2^T(t)Q_{22}e_2(t) \\ &= (e_2(t) + Q_{22}^{-1}Q_{21}e_1(t))^T Q_{22}(e_2(t) + Q_{22}^{-1}Q_{21}e_1(t)) \\ &\quad - e_1^T(t)Q_{21}^T Q_{22}^{-1}Q_{21}e_1(t), \end{aligned}$$

(7) can be rewritten in the form of

$$J = \tfrac{1}{2}\int_{t_s}^{\infty} \left(e_1^T(t)\overline{Q}e_1(t) + \upsilon^T(t)Q_{22}\upsilon(t)\right) dt,$$

where

$$\begin{aligned} \overline{Q} &= Q_{11} - Q_{12}Q_{22}^{-1}Q_{21}, \\ \upsilon(t) &= e_2(t) + Q_{22}^{-1}Q_{21}e_1(t). \end{aligned}$$

Based on the LQR minimisation of J in association with the nominal system in (5), we obtain

$$\upsilon(t) = -Q_{22}^{-1}A_{12}^T Pe_1(t),$$

where P satisfies the following equation

$$\mathcal{A}^T P + P\mathcal{A} - PA_{12}Q_{22}^{-1}A_{12}^T P + \overline{Q} = 0,$$

in which $\mathcal{A} = A_{11} - A_{12}Q_{22}^{-1}Q_{21}$ and A_{ij} is the subblocks obtained from partitioning matrix $\overline{A}$ in (5). Consequently, we obtain

$$e_2(t) = -Q_{22}^{-1}(A_{12}^T P + Q_{21})e_1(t). \quad (8)$$

During the sliding motion, we have $s(t) = 0$ so that

$$e_2(t) = Ce_1(t). \quad (9)$$

Thus, by comparing (8) and (9), the design matrix of the sliding function is obtained explicitly as

$$C = Q_{22}^{-1}(A_{12}^T P + Q_{21}). \quad (10)$$

3.4 Robust optimal sliding mode control

Before presenting our proposed control scheme, the following definition and lemma are introduced.

Definition 1: The solution of system (5) is uniformly exponentially convergent to a ball $B(0,r) = \{e \in \mathbb{R}^n : \|e\| \le r\}$ with rate $\gamma > 0$ if for any $\xi > 0$, there exists $k(\xi) > 0$ such that

$$\|e(t)\| \le r + k(\xi)\exp(-\gamma t), \ \forall t \ge 0.$$

Lemma 1: [18] Let $V(t)$ be a continuous positive definite function for all $t \ge 0$, $k^* \ge 0$ and

$$\dot{V}(t) \le -\eta V(t) + \nu, \ \forall t \ge 0,$$

where η and ν are positive constants, then

$$\dot{V}(t) \le r + k^* \exp(-\gamma t), \ \forall t \ge 0,$$

in which $r = \nu/\eta$ and $\gamma = \eta$ is the exponential convergence rate.

The control scheme proposed here has the form of

$$u(t) = u_E(t) + u_R(t), \quad (11)$$

where $u_E(t)$ and $u_R(t)$ are respectively the equivalent and switching control. The equivalent control which maintains the sliding motion on the sliding surface is defined as $u_E(t) = u_{E_1}(t) + u_{E_2}(t)$ where

$$u_{E_1}(t) = -(\overline{C}\overline{B})^{-1}\left(\overline{C}\overline{A}_d e(t) + \Pi s(t)\right), \quad (12)$$

and

$$u_{E_2}(t) = \overline{K}z(t) + Lr_d(t), \quad (13)$$

in which Π is a design diagonal matrix with real distinct positive eigenvalues and $\overline{K} = KT^{-1}$. For a given convergence ball radius r_0, the following switching control $u_R(t)$ is designed to force the system trajectories towards the prescribed sliding surface

$$u_R(t) = -(\overline{C}\overline{B})^{-1}\frac{\mu s(t)}{\|s(t)\| + \varepsilon}, \quad (14)$$

where

$$\mu = \frac{2r_0\lambda_{\min}(\Pi)}{\varepsilon}$$

and $\varepsilon > 0$ is a small positive scalar for chattering reduction to be selected according to the theorem stated below.

Theorem 1: For with given bounds of the system uncertainty β and disturbance $\overline{\omega}_p$ and radius r_0, the state trajectories of offshore container crane system (4) are driven towards the sliding function designed as in (6) under the following control law

$$\begin{aligned} u(t) = &-(\overline{C}\overline{B})^{-1}\left(\overline{C}\overline{A}_d e(t) + \Pi s(t) + \frac{\mu s(t)}{\|s(t)\| + \varepsilon}\right) \\ &+ \overline{K}z(t) + Lr_d(t), \end{aligned} \quad (15)$$

where ε is chosen to be sufficiently small such that

$$\varepsilon \leq \frac{2r_0\lambda_{\min}(\Pi)}{\|\overline{C}\,\overline{D}\|\overline{\omega}_p + \beta\|\overline{C}\|\|z(t)\|}. \tag{16}$$

Proof: Consider the Lyapunov function

$$V = \tfrac{1}{2}s^T(t)s(t).$$

By taking its derivative along the solutions of (5), we obtain

$$\begin{aligned}\dot{V}(t) &= s^T(t)\Big(\overline{C}\,\Delta\overline{A}(t)z(t) - \Pi s(t) \\ &\quad - \frac{\mu s(t)}{\|s(t)\| + \varepsilon} + \overline{C}\,\overline{D}\omega(t)\Big) \\ &\leq -\lambda_{\min}(\Pi)\|s(t)\|^2 + \beta\|\overline{C}\|\|z(t)\|\|s(t)\| \\ &\quad - \frac{\mu\|s(t)\|^2}{\|s(t)\| + \varepsilon} + \|\overline{C}\,\overline{D}\|\|s(t)\|\overline{\omega}_p.\end{aligned}$$

From (16), we obtain

$$\mu \geq \beta\|\overline{C}\|\|z(t)\| + \|\overline{C}\,\overline{D}\|\overline{\omega}_p.$$

Thus,

$$\begin{aligned}\dot{V}(t) &\leq -\lambda_{\min}(\Pi)\|s(t)\|^2 + \Big(\beta\|\overline{C}\|\|z(t)\| \\ &\quad + \|\overline{C}\,\overline{D}\|\overline{\omega}_p\Big)\frac{\|s(t)\|\varepsilon}{\|s(t)\| + \varepsilon}.\end{aligned}$$

Consequently, by using inequalities $\frac{ab}{a+b} \leq b, \forall a, b > 0$, we obtain the following inequality

$$\dot{V}(t) \leq -2\lambda_{\min}(\Pi)V(t) + \Big(\beta\|\overline{C}\|\|z(t)\| + \|\overline{C}\,\overline{D}\|\overline{\omega}_p\Big)\varepsilon.$$

Thus, from Definition 1 and Lemma 1, we get

$$V(t) \leq r_0 + k_1\exp(-\gamma t), \quad \forall t \geq 0,$$

where

$$r_0 = \frac{\Big(\beta\|\overline{C}\|\|z(t)\| + \|\overline{C}\,\overline{D}\|\overline{\omega}_p\Big)\varepsilon}{2\lambda_{\min}(\Pi)},$$

and $\gamma = 2\lambda_{\min}(\Pi)$. The proof is completed.

4 Results and Discussion

In this study, numerical values of the offshore container crane system parameters are listed as $m_c = 6 \times 10^3$ kg, $m_p = 20 \times 10^3$ kg, $h = 10$ m, $K_{cy} = 600$ N/m.s^{-1}, $K_{cl} = 200$ N/m.s^{-1}, $K_{c\theta} = 100$ N.m/rad.s^{-1} and $g = 9.81$ m.s^{-1}. The nominal state vector is chosen as $x_0 = [10\text{ m}, 8\text{ m}, 0, 0, 0, 0, 0]^T$, which provides $u_0 = [0, -196.14]^T$ kN. For the sake of illustration, the following parameters are provided as $l_D = 10$ m , $l_U = 4$ m, $v_R = 3$ m/s, $v_y = 0.63$ m/s, $y_F = 10$ m. The values of the constants in $\omega(t)$ are listed as as $F_{cy} = 5$ kN, $F_{cl} = 2$ kN, $\tau_{c\theta} = 2$ kN.m, $\rho_w = 1.225$ kg/m^3, $v_w = 15$ m/s, $c_d = 1.05$, $A_p = 12$ m^2, and $L_c = 1.2$ m. The heaving acceleration and the rolling angular displacement

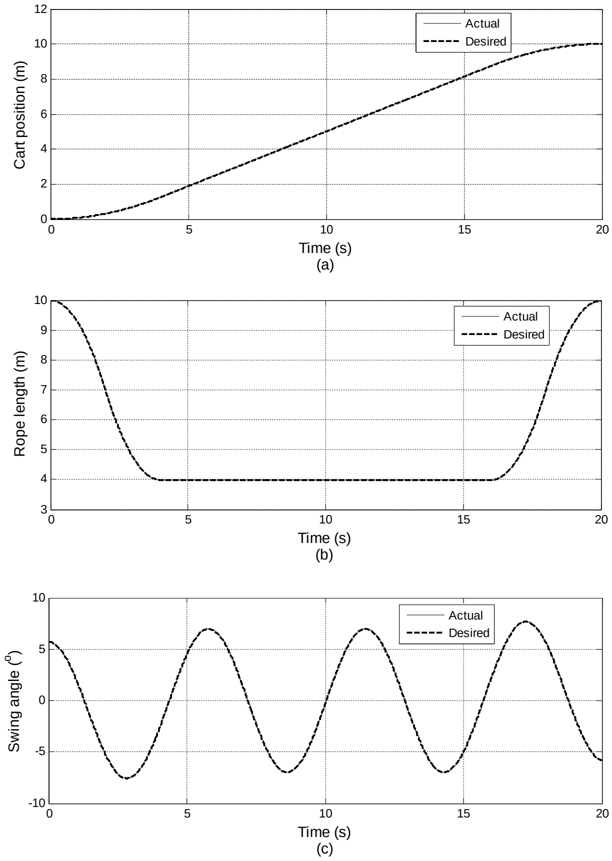

Figure 2: Trajectory tracking responses of the (a) cart position; (b) rope length; and (c) swing angle.

of the vessel to accommodate ocean waves in an allowable range are assumed to be respectively $\ddot{\zeta}(t) = 0.4\sin t$ m/s^2 and $\alpha(t) = \frac{\pi}{36}\cos t$ rad [19]. The details of matrices A, $\Delta A(t)$, B, D, K and L are then listed as follows:

$$A = \begin{bmatrix} 0 & 0 & 0 & 1 & 0 & 0 \\ 0 & 0 & 0 & 0 & 1 & 0 \\ 0 & 0 & 0 & 0 & 0 & 1 \\ 0 & 0 & 3.270 & -0.01 & 0 & 0.0021 \\ 0 & 0 & 0 & 0 & -0.001 & 0 \\ 0 & 0 & -5.314 & 0.0125 & 0 & -0.0034 \end{bmatrix},$$

$$\Delta A = \begin{bmatrix} 0_{3\times 3} & 0_{3\times 3} \\ \Psi & 0_{3\times 3} \end{bmatrix},$$

$$\Psi = \begin{bmatrix} 3.33\dot{\alpha}^2 & 0 & \Psi_{13} \\ 0 & \dot{\alpha}^2 & 0.98\sin\alpha \\ 0 & 0 & \Psi_{33} \end{bmatrix},$$

$$\Psi_{13} = 6\dot{\alpha}^2 - \ddot{\alpha} + (0.98 + 0.1\ddot{\zeta})\cos\alpha,$$

$$\Psi_{33} = -8.75\dot{\alpha}^2 + 5.42\ddot{\alpha} - (5.31 + 0.54\ddot{\zeta})\cos\alpha,$$

$$B = \begin{bmatrix} 0 & 0 & 0 & 0 & 1.667 & 0 & -2.083 \\ 0 & 0 & 0 & 0 & 0 & 0.5 & 0 \end{bmatrix}^T,$$

$$D = \begin{bmatrix} 0_{3\times 3} \\ D_2 \end{bmatrix},$$

$$D_2 = \begin{bmatrix} -1.667 & 0 & 2.083 \\ 0 & -0.5 & 0 \\ 2.083 & 0 & -2.604 \end{bmatrix},$$

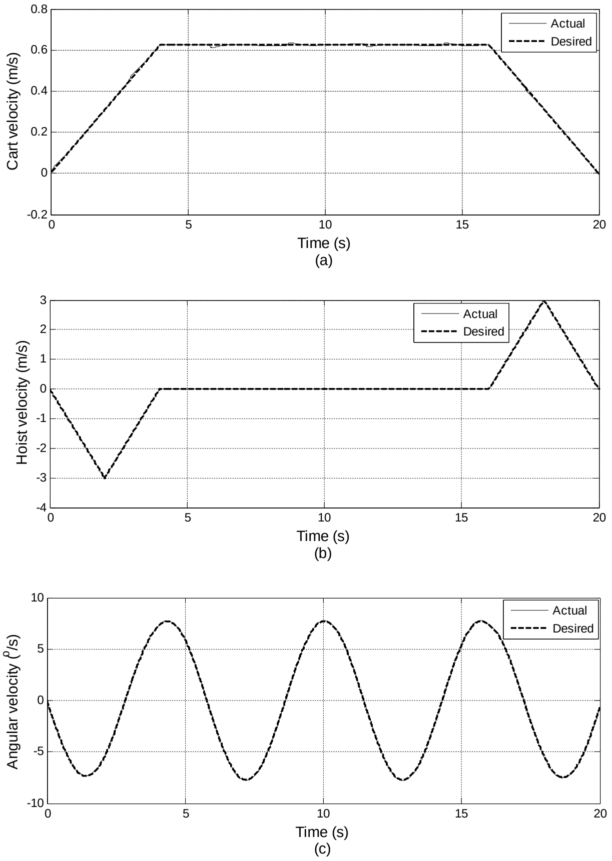

Figure 3: Trajectory tracking responses of the (a) cart velocity; (b) hoist velocity; and (c) swing angular velocity.

$$K = \begin{bmatrix} 0 & 0 & -1.962 & 0.006 & 0 & -0.0013 \\ 0 & 0 & 0 & 0 & 0.002 & 0 \end{bmatrix},$$

$$L = \begin{bmatrix} 1 & 0 \\ 0 & 1 \end{bmatrix}.$$

The transformation matrix is obtained as

$$T = \begin{bmatrix} 0 & 0 & 1 & 0 & 0 & 0 \\ -0.625 & 0 & 0 & 0.610 & 0 & 0.488 \\ 0 & -1 & 0 & 0 & 0 & 0 \\ 0.781 & 0 & 0 & 0.488 & 0 & 0.390 \\ 0 & 0 & 0 & -0.625 & 0 & 0.781 \\ 0 & 0 & 0 & 0 & -1 & 0 \end{bmatrix}.$$

Using the quadratic minimisation, the state weighting matrix Q is chosen as $Q = TRT^{-1}$, $R = \mathrm{diag}(10, 10, 5, 1, 1, 1)$ which provides the following matrix $\overline{C}$:

$$\overline{C} = \begin{bmatrix} 1.798 & -0.949 & 0 & -4.809 & 1 & 0 \\ 0 & 0 & 3.162 & 0 & 0 & 1 \end{bmatrix}.$$

The upper bounds of the system disturbance $\overline{\omega}_p$ and uncertainty β are *a priori* selected as 0.5 and 5.8 respectively. From Theorem 2, by choosing the exponential decay rate $\gamma = 30$, radius $r_0 = 0.004$ for the sliding surface trajectories $s(t)$ and $\varepsilon = 0.0025$, we obtain $\mu = 48$.

The displacements and velocities of the cart position and rope length are assigned to track the trajectories as defined in Section 3. Aside from that, it can be shown that if the swing angle tracks the roll angle of the vessel during the operation process, the payload will be held on the vertical plane in the frame $\{O_0x_0y_0z_0\}$. Therefore, the desired payload swing trajectory is chosen as $\theta_d(t) = \alpha(t)$. Figure 2 depicts the trajectory tracking responses of cart position, rope length and swing angle and Figure 3 depicts the trajectory tracking responses of the corresponding velocities. Continuous small oscillations are occurred in the cart position and its corresponding velocity due to the persistent rolling vibration-induced motion of the vessel. This continuous small oscillation is apparent in the cart velocity response of Figure 3(a) during the container placement stage (Stage 2). However, the rope length response is less affected by the presence of heaving motion of the vessel owing to robustness of the control system.

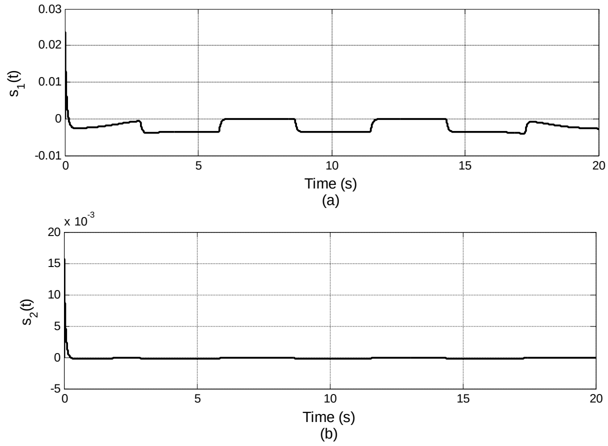

Figure 4: Switching functions.

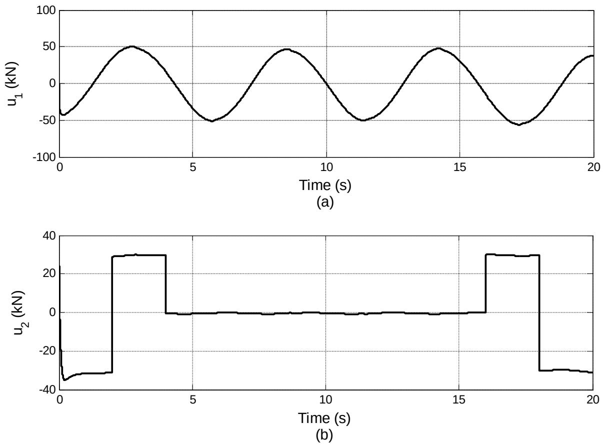

Figure 5: Input forces.

Figure 4 shows the plot of switching functions and Figure 5 shows the control forces of the system. The effect of persistent rolling vibration-induced motion of the vessel can also be seen in the responses of both $s_1(t)$ and $u_1(t)$. Based on the quadratic minimisation approach, $s_1(t)$ consists of the coupled motion of the cart and the swing angle whereas $s_2(t)$ corresponds to the rope length dynamics. Overall, based on Figure 2(a)-(b) and Figure 3(a)-(b), an excellent decoupling of the cart position and swing angle is exhibited.

5 Conclusion

In this paper, the problem of robust sliding mode control for offshore container crane systems with bounded disturbances and uncertainties has been addressed. By taking the effects of payload mass and length of rope changes as well as vibrations induced by ocean waves and gusty winds into account, the mathematical model of offshore container crane systems is derived for the first time. An LQR-based design approach is developed to obtain the sliding surface to achieve the optimal performance of the equivalent dynamics. To track the crane's desired trajectory, robust sliding mode control law is then designed to drive the state variables of the system towards the sliding surface in finite time and maintain them on that surface after subsequent time. Extensive simulation results are provided to demonstrate good tracking performance of the proposed controller for offshore crane systems in dealing with the harsh open-sea conditions.

References

[1] A.V. Goodchild and G.F. Daganzo, "Crane double cycling in container ports: Planning methods and evaluation," *Transportation Research Part B: Methodological*, vol. 41, no. 8, pp. 875-891, 2007.

[2] G.Y. Ke, K.W. Li, and K.W. Hipel, "An integrated multiple criteria preference ranking approach to the Canadian west coast port congestion conflict," *Expert Systems with Applications*, vol. 39, pp. 9181-9190, 2012.

[3] L. Fan, W.W. Wilson, and B. Dahl, "Congestion, port expansion and spatial competition for US container imports," *Transportation Research Part E: Logistics and Transportation Review*, vol. 48, no. 6, pp. 1121-1136, 2012.

[4] E. Lataire, M. Vantorre, G. Delefortrie, and M. Candries, "Mathematical modelling of forces acting on ships during lightering operations," *Ocean Engineering*, vol. 55, pp. 101-115, 2012.

[5] Q. Ngo and K. Hong, "Sliding-mode antisway control of an offshore container crane," *IEEE/ASME Trans. Mechatronics*, vol. 17, no. 2, pp. 201-209, 2012.

[6] X.F. Yin, L.P. Khoo, and C-H. Chen, "A distributed agent system for port planning and scheduling," *Journal of Advanced Engineering Informatics*, vol. 25, no. 3, pp. 101-115, 2011.

[7] Z.N. Masoud and M.F. Daqaq, "A graphical approach to input-shaping control design for container crane with hoist," *IEEE Transactions on Control Systems and Technology*, vol. 14, no. 6, pp. 1070-1077, 2006.

[8] S. Garrido, M. Abderrahim, A. Gimenez, R. Diez, and C. Balaguer, "Antiswinging input shaping control of an automatic construction crane," *IEEE Transactions on Automation Science and Engineering*, vol. 5, no. 3, pp. 549-557, 2008.

[9] M. Borsc, A. Vitko, and B. Thursky, "Optimal stabilization of modal control with variable structure," *Transactions on Instrument Measurement Control,* vol. 30, no. 1, pp. 63-76, 2008.

[10] K. Terashima, Y. Shen, and K. Yano, "Modeling and optimal control of a rotary crane using the straight transfer transformation method," *Control Engineering Practice,* vol. 15, no. 9, pp. 1179-1192, 2007.

[11] C.Y. Chang, "Adaptive fuzzy controller of the overhead cranes with nonlinear disturbance, " *IEEE Transactions on Industrial Informatics*, vol. 3, no. 2, pp. 164-172, 2007.

[12] Q.P. Ha, Q.H. Nguyen, D.C. Rye, and H.F. Durrant-Whyte, "Impedance control of a hydraulically actuated robotic excavator," *Automation in Construction*, vol. 9, pp. 421-435, 2000.

[13] H.-S. Choi, C.-S. Han K. Lee, and S. Lee, "Development of hybrid robot for construction works with pneumatic actuator," *Automation in Construction*, vol. 14, pp. 452-459, 2005.

[14] Y. Ming, S. Wei, and H. Ping, "Dynamic coordinated control of attitude correction for the shield tunneling based on load observer," *Automation in Construction*, vol. 24, pp. 24-29, 2012.

[15] R.M.T.R. Ismail and Q.P. Ha, "Second-order Sliding Mode Control for Offshore Container Crane," *Proceeding of Australasian Conference on Robotics and Automation*, Victoria University of Wellington, New Zealand, 2012.

[16] R.M.T.R. Ismail and Q.P. Ha, "Trajectory Tracking and Anti-sway Control of Three-dimensional Offshore Boom Cranes Using Second-order Sliding Modes," *Proc. IEEE Int. Conf. on Automation Science and Engineering*, Madison WI, USA, pp. 996-1001, 2013.

[17] P.K. Kundu, I.M. Cohen, and D.R. Dowling, *Fluid Mechanics*, Academic Press, New York, 2012.

[18] S. Oucheriah, "Robust exponential convergence of a class of linear delayed systems with bounded controllers and disturbances," *Automatica*, vol. 42, no. 11, pp. 1863-1867, 2006.

[19] Y. Fang, P. Wang, N. Sun, and Y. Zhang, "Dynamics analysis and nonlinear control of an offshore boom crane," *IEEE Trans. Industrial Electronics*, vol. 61, no. 1, pp. 414-427, 2014.